Journal of Cellular Biochemistry 94:433–445 (2005)

ARTICLES

Lysosomal and Mitochondrial Pathways in H_2O_2-Induced Apoptosis of Alveolar Type II Cells

Lei Yin, Rebecca Stearns, and Beatriz González-Flecha*

Physiology Program, Department of Environmental Health, Harvard School of Public Health, Boston, Massachusetts

Abstract Increasing evidence suggests a role for apoptosis in the maintenance of the alveolar epithelium under normal and pathological conditions. However, the signaling pathways modulating alveolar type II (AT II) cell apoptosis remain poorly defined. Here we investigated the role of lysosomes as modulators of oxidant-mediated AT II cell apoptosis using an in vitro model of H_2O_2-stress. H_2O_2 stress led to time-dependent increases in intracellular oxidants, mitochondrial membrane polarization, cytochrome *c* release, lysosomal rupture, and AT II cells apoptosis. Increased apoptosis was prevented by specific inhibition of the caspase cascade using the broad-spectrum caspase inhibitor z-VAD-fmk or a caspase 3 inhibitor, or by using functional inhibitors for cathepsin D (pepstatin A) or cathepsin B. Inhibition of cathepsin D also prevented mitochondrial permeabilization and cythocrome *c* release suggesting that lysosomal rupture precedes and is necessary for the activation of the mitochondrial pathway of cell death. J. Cell. Biochem. 94: 433–445, 2005.

Key words: hydrogen peroxide; alveolar type II cells; apoptosis; lysosomes

The lung is a primary target for oxygen toxicity because of its constant exposure to high oxygen levels and environmental oxidants. Reactive oxygen species ((ROS): superoxide anion (O_2^-), hydrogen peroxide (H_2O_2), hydroxyl radical ($HO^\cdot$); and singlet oxygen ($^1O_2$)) have been implicated as mediators of the lung injury associated with supplemental oxygen therapy [Kelly and Lubec, 1995] and to several environmental exposures [Gurgueira et al., 2002] and occupational lung diseases like silicosis and asbestosis [Ryrfeldt and Bannenberg, 1993; Vallyathan and Shi, 1997].

Increasing evidence suggests a role for apoptosis in the maintenance of the alveolar epithelium under normal and pathological conditions. Alveolar type II (AT II) cells undergo apoptosis during normal development and maturation of the lungs [Nishino et al., 1999], and in association with acute lung injury [Bardales et al., 1996]. However, the signal transduction pathways modulating AT II cell apoptosis remain poorly defined.

Apoptosis is a widespread phenomenon by which cells are eliminated in response to activation of an intrinsic program. Apoptosis is characterized morphologically by cellular shrinkage and chromatin condensation, and biochemically by the coordinated activation of specific signaling pathways. Accumulating evidence suggests that, not only mitochondria, but also lysosomes, endoplasmic reticulum, and the Golgi apparatus play major roles in damage sensing or integration of apotptotic signaling [Ferri and Kroemer, 2001].

Apoptotic signaling can be triggered by a variety of extracellular stimuli, such as radiation, oxidants, cytokines, growth factor withdrawal, etc. Induction of apoptosis by ROS in vitro has been reported in a variety of cell lines, including immortalized lung epithelial cells from rats (RLE) and humans (A549) [Janssen et al., 1997; Ye et al., 1999], and primary cultures of AT II cells [Carvalho et al., 2004]. Exposure to submillimolar levels of H_2O_2

Grant sponsor: NIH; Grant numbers: RO1 HL/ES68073, P50 ES00002.

*Correspondence to: Beatriz González-Flecha, Physiology Program, SPH2-213, Department of Environmental Health, 665 Huntington Ave., Boston, MA 02115.
E-mail: bgonzale@hsph.harvard.edu

Received 10 June 2004; Accepted 19 July 2004

DOI 10.1002/jcb.20277

has been shown to induce apoptosis in a variety of cells and by mechanisms involving either a mitochondrial cytochrome *c*-dependent pathway [Brookes et al., 2002] or a lysosome-mediated pathway [Brunk et al., 1995; Antunes et al., 2001]. Recent reports have indicated that enzymes such as cathepsins D and B are translocated from lysosomal compartments to the cytosol early during apoptosis and that translocation of cathepsins D and B occur before cytochrome *c* release and caspase activation [Guicciardi et al., 2000; Dare et al., 2001].

In this study, we used a model of acute H_2O_2 stress in primary AT II cells to investigate the possible involvement of the lysosomes in H_2O_2-induced apoptosis in the lung epithelium.

MATERIALS AND METHODS

Reagents

Rat IgG, hydrogen peroxide was purchased from Sigma Chemical Co. (St. Louis, MO). Elastase was from Worthington Biochemical. Dulbecco's modified Eagle's medium, vitamins; fetal bovine serum and newborn calf serum were from Gibco Laboratories (Grand Island, NY). Rabbit polyclonal antibodies against cytochrome *c* (H-104) and GAPDH were from Santa Cruz Biotechnology (Santa Cruz, CA). Benzyloxycarbonyl-Val-Ala-Asp-fluoromethyl ketone (zVAD-fmk), a broad-spectrum caspase inhibitor (Caspase Inhibitor I), acetyl-Asp-Met-Gln-Asp-aldehyde a specific inhibitor of caspase-3 (Ac-DMQD-CHO, caspase-3 Inhibitor IV), the cathepsin D inhibitor Pepstatin A, and the Cathepsin B inhibitor acetyl-Leu-Val-lysinal (Ac-LVK-CHO) a lysinal analog of Leupeptin were from Calbiochem (La Jolla, CA). 3,3′-dihexyloxacarbocyanine iodide (DiOC6), 2′,7′-dichlorodihydrofluorescein diacetate (DCFH-DA), acridine orange (AO), pepstatin A BODIPY® FL conjugate, MitroTracker Red CMXRos were from Molecular Probes (Eugene, OR).

Alveolar Type II Cell Isolation

AT II cells were isolated from pathogen-free Sprague Dawley rats weighing 180–220 g using the method of Dobbs [1990], as described [González-Flecha et al., 1996]. Rats were anesthetized with sodium pentobarbital (50 mg/kg body weight) and the heart and lungs were rapidly removed. Lungs were perfused via the pulmonary artery, lavaged and incubated with elastase solution (30 U/ml) for 20 min at 37°C. The tissue was then minced and filtered through sterile filters of 120 and 20 μm nylon mesh. AT II cells were purified by differential adherence to IgG coated plates. AT II cells were suspended in Dulbecco's modified Eagle's medium (DMEM) containing 10% fetal bovine serum, vitamins, 2 mM glutamine, 40 mg/ml gentamicin, 100 U/ml penicillin, and 100 μg/ml streptomycin. Viability of the final preparation, assayed by exclusion of Trypan blue, was higher than 90%. Cells were used the day next to isolation. Purity of the cells was $\geq$95% as assessed by Papanicolaou staining [Dobbs, 1990].

Cell Culture and Treatment

Primary AT II cells were plated immediately after isolation at a density of 10^6 cells/cm^2. Cells were cultured in DMEM (supplemented as described above) in a humidified atmosphere of 5% CO_2–95% air at 37°C. After 24 h, non-adherent cells were removed by replacing the medium. Primary AT II cells were then treated according to each protocol. We studied the time course of induction of apoptosis induced by H_2O_2, by treating the cells with single dose of 50 μM H_2O_2.

Apoptosis

Apoptotic cells were identified as the sub-G_1 peak of the DNA content profiles after propidium iodide staining [Chen et al., 1996]. Briefly, cells were harvested by trypsinization, resuspended with 70% ethanol/PBS, and stored at 4°C until analysis. Cells were then stained with 50 mg/ml propidium iodide for 1 h in the presence of 40 mg/ml of RNAse A (DNAse-free). For the determinations of apoptosis, a total of 10^4 cells were counted. Measurements were carried out in a Coulter Flow Cytometer (Beckman Coulter, Fullerton, CA). The light source was a 15 mW argon laser exciting at 488 nm. The fluorescence intensity of PI-DNA was detected at an emission wavelength of 610 nm and quantified as relative channel numbers in FL4. The sample flow and data rate was set respectively at 35 μl/min and 50–80 events/s.

Intracellular ROS Levels

Changes in intracellular ROS concentrations were assessed with a method adapted from Bass et al. [Bass et al., 1983]. Briefly, AT II cells were plated in a 96 wells plate, grown overnight, and loaded for 30 min with 20 μM 2′-7′ dichlorofluorescein diacetate (DCFH-DA). The cells

were then rinsed twice with PBS and treated with H_2O_2. DCF fluorescence (excitation 488 nm, emission 575 nm) was measured by flow cytometry 15, 30, and 60 min after addition of H_2O_2. A total of 10^4 cells were counted.

Determination of Mitochondrial Transmembrane Potential

The mitochondrial transmembrane potential ($\Delta\psi$), was measured using the cationic lipophilic fluorochrome 3,3′-dihexyloxacarbocyanine iodide (DiOC6). DIOC6 is distributed on the mitochondrial matrix following the Nernst equation and therefore correlating with $\Delta\psi$. DiOC6 can be therefore used to measure variations in the $\Delta\psi$ m on a per-cell basis. 10^6 cells were loaded with 1 nM DiOC6 in PBS for 20 min at room temperature, washed twice with cold PBS, and immediately analyzed by flow cytometry.

Lysosomal Stability

Cells were assessed for lysosomal stability using the acridine orange (AO) relocation methods [Antunes et al., 2001]. AO is a lysosomotropic base and a metachromatic fluorochrome exhibiting red fluorescence when highly concentrated and green fluorescence at low concentration. In order to detect early and minor lysosomal destabilization, we therefore followed increases in green fluorescence, corresponding to redistribution of AO in the cytoplasm. 10^6 cells were stained with 5 μg/ml AO for 15 min at 37°C, washed, resuspended in complete medium, and treated with 50 μM H_2O_2. H_2O_2 treatment and harvesting were done in dark. Increases in green fluorescence (488 nm) were measured by flow cytometry.

Western Blot Analysis for Cytochrome *c*

Cells (20×10^6) were collected at the indicated times and washed twice in ice-old PBS buffer. Cell pellets were resuspended in cytosol extraction buffer (containing 200 mM manitol, 68 mM sucrose, 50 mM PIPES–KOH, 50 mM KCl, 5 mM EGTA, 2 mm $MgCl_2$, 1 mM DTT, and protease inhibitors (Complete Cocktail). After 30 min incubation on ice, cells were homogenized with a dounce homogenizer, the homogenate was spun at 14,000*g* for 15 min, and supernatants were removed and stored at −80°C until analysis [Pervaiz et al., 1999]. Cytochrome *c* levels were determined by Western blot. Fifty micrograms of cytosolic fractions were resolved on 18% SDS-polyacrylamide gels and blotted onto nitrocellulose (PVDF). Membranes were then blocked overnight with 5% dry milk in TBST (50 mM Tris/HCl, 150 mM NaCl, 0.1% Tween 20), incubated for 1 h with primary anti-cytochrome *c* and anti-caspase 3 antobodies at room tempterature (dilution 1:5,000 in TBS with 0.0055% Tween 20 and 1% BSA), washed three times with TBST, and incubated for 1 h with goat anti-rabbit IgG-horseradish peroxidase (HRP) conjugate (dilution 1:5,000). Immunoreactive bands were visualized using enhanced chemiluminescence (Pierce, Rockford, IL) and BioMax films (Kodak, New Haven, CT). The densitometric analysis of the films was performed on a Macintosh computer (Apple, Cupertino, CA). The blots were then stripped and reprobed with Actin as loading control.

Confocal Laser Scanning Microscopy

For confocal microscopy, 10^6 cells were cultured on glass-bottomed Lab-Tek Chamber Slides (Nalge Nunc, Naperville, IL). Monolayers of living cells were loaded with 20 nM MitoTracker Red CMXRos (mitochondrial membrane potential) and 20 nM pepstatin A BODIPY® FL conjugate (cathepsin D trafficking) for 1 h at 37°C in complete culture medium. After loading, cells were washed twice with complete culture medium and treated with 50 μM H_2O_2. Cells were examined using a Leica TCSNT confocal laser scanning microscope (Leica Inc., Exton, PA) fitted with air-cooled argon and krypton lasers. Fields were selected at random and the cells brought into focus under bright-field conditions. Flurorescent confocal micrographs were recorded under dual fluorescent imaging mode in which specimens were simultaneously exposed to 488 and 568 nm light attenuated by an acusto-tunable optical filter. A band pass filter was used to select light emitted from the MitoTracker Red and a long pass 590 nm filter to detect the BODIPY labeled probe. Serial sections were collected from the apical surface at 0.049 μm pixel size, with a step increment of 0.2 μm in the Z-axis. Images are presented without filtering as a two-color composite in which MitoTracker Red appears as red and BODIPY as green. In those locations where staining for MitoTracker Red and BODIPY are superimposed, labeling appears yellow.

Electron Microscopy

For transmission electron microscopy (TEM), 10^7 cells were treated with 50 μM H_2O_2 in suspension. At the indicated times, cells were spun down, rinsed with PBS, and fixed with glutaraldehyde in cacodylate buffer. Subsequent osmication was done in 1% osmium tetroxide in cacodylate buffer and dehydrated in ascending series of alcohol (25, 50, 75, 95%) for 10 min each, and in 100% 2 times 10 min each. After dehydration, the cells were infiltrated with araldite:ethanol (1:1) for 2 h, araldite:ethanol (4:1) overnight, araldite for 45 min at 45°C, araldite for 45 min at 55°C, and finally araldite to a depth of 1.5–2 mm before polymerisation at 60°C overnight. Ultrathin sections (30 nm) of pale gold coloration cut from these blocks by an RMC MT6000 ultramicrotome (RMC, Inc., Tucson, AZ) were collected onto 600-meshed copper grids, which were supported with Formvar films. The sections on the grids were examined in a LEO EM902 energy-filtering transmission electron microscope (Leo Electron Microscopy, Inc., Thornwood, NY).

Statistical Analysis

Values are expressed as the mean value of at least three experiments ±standard error of the mean (SEM). Mean values were compared by using ANOVA followed by Dunnet's or Fisher's test for comparison of the means, using the Statview 4.5 software (Abacus Conceptes, Berkeley, CA). The figures illustrate representative patterns of at least three experiments.

RESULTS

Inhibition of the Caspase Cascade and Lysosomal Activation Prevents H_2O_2-Induced Apoptosis in Alveolar Epithelial Cells

Flow cytometry analysis of cell cycle position in untreated primary cultures of AT II cells showed that $8 \pm 3\%$ of the cell population corresponded to sub-G1, apoptotic cells (Fig. 1A). After 16 h of treatment with 50 μM H_2O_2 the percentage of apoptotic cells was significantly increased with average maximal values of $50 \pm 10\%$ ($P < 0.01$ as compared to control).

As a first approach to study the mechanisms underlying H_2O_2-induced apoptosis in this cell type we use a panel of inhibitors that block different steps of the caspase cascade, as well as lysosomal activation. Cells treated with the pan caspase inhibitor zVAD-fmk (Fig. 1C, 10 μM) showed no increase in the percentage of apoptotic cells in response to H_2O_2 ($7 \pm 4\%$, $P < 0.01$ as compared to H_2O_2-treated). Inhibition of caspase 3 with caspase-3 inhibitor IV (Fig. 1D) also showed partial inhibition of H_2O_2-induced apoptosis ($24 \pm 7\%$, $P > 0.05$ as compared to H_2O_2-treated). Similarly, AT II cells treated with the lysosomal aspartic proteinase inhibitor Pepstatin A (Fig. 1E) showed a diminished response to H_2O_2 treatment ($13 \pm 5\%$, $P < 0.05$ compared to H_2O_2), while cells treated with the cathepsin B inhibitor II (Fig. 1F) responded to H_2O_2 exposure as control cells ($37 \pm 8\%$, $P > 0.05$).

H_2O_2 Treatment Increases Intracellular Oxidants

We follow the time course of increase in intracellular oxidants by using the cell permeable fluorescent probe 2′,7′-dichlorodihydrofluorescein diacetate (DCFH-DA [Sigaud et al., 2004]). H_2O_2-treated AT II cells were followed for DCFH oxidation for 0–60 min (Fig. 2). Our data shows significant increases in intracellular oxidants 15 min (220 ± 30, control 140 ± 10, $P < 0.05$), 30 min (460 ± 60, $P < 0.01$), and 60 min (420 ± 30, $P < 0.01$) after addition of H_2O_2.

Mitochondrial Alterations in H_2O_2 Treated AT II Cells

The data in Figure 1 show that both mitochondrial and lysosomal pathways are involved in H_2O_2-induced apoptosis. To further characterize the role of each of these pathways we evaluated markers of mitochondrial apoptotic signaling and lysosomal activation.

Mitochondrial involvement was evaluated by following changes on the mitochondrial transmembrane potential (Fig. 3) and release of mitochondrial cytochrome *c* (Fig. 4) after H_2O_2 treatment. Reductions in mitochondrial transmembrane potential (MMP) are early markers of apoptosis (Fig. 3), and the decline of membrane potential reflect the opening of permeability transition pores, which in turn results in mitochondrial swelling and rupture of the outer mitochondrial membrane with the release of cytochrome *c* from the intermembrane space of the mitochondrial into the cytoplasm.

The fluorescence intensity of DiOC6 (a marker of MMP) was significantly decreased in H_2O_2-treated AT II cells 30 min after stimulation (Fig. 3, $22 \pm 12\%$, control $93 \pm 4\%$, $P < 0.01$).

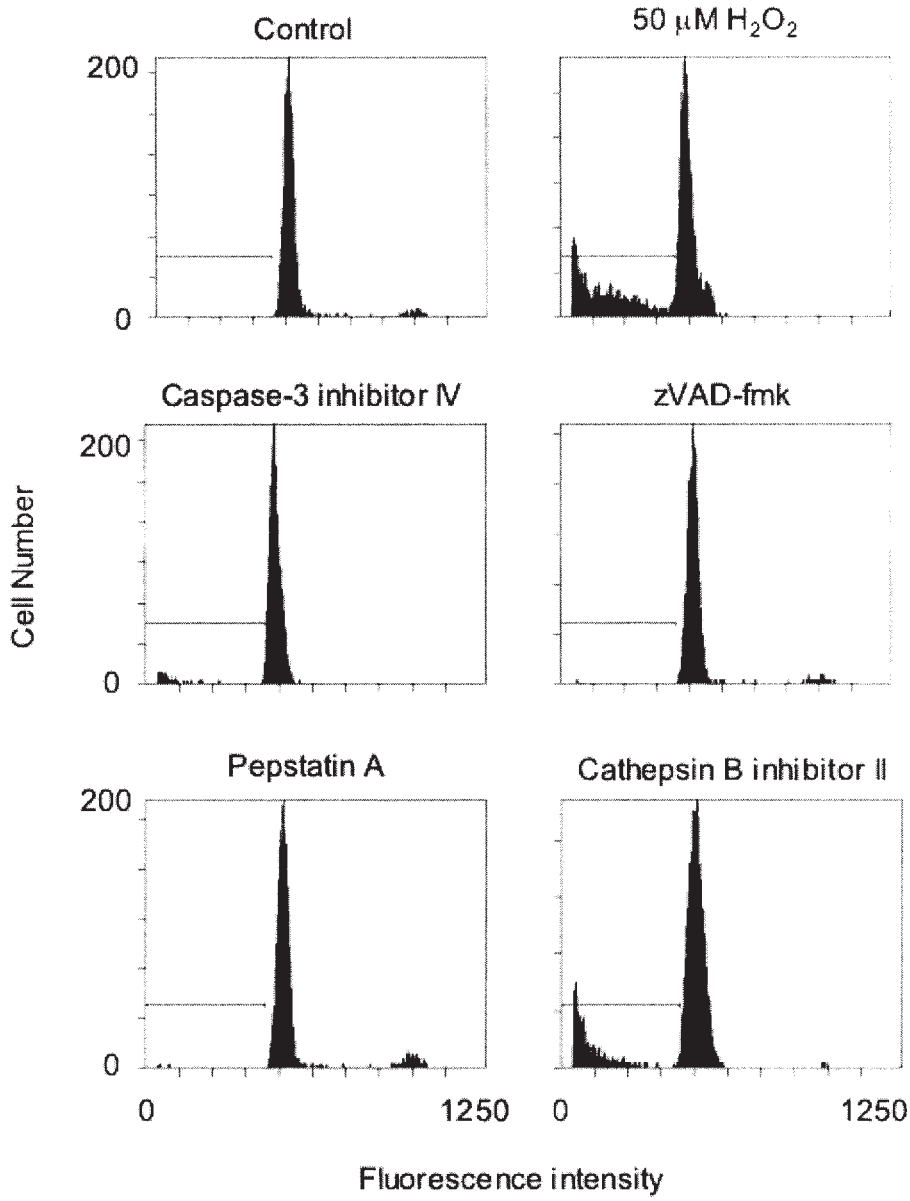

Fig. 1. Cell cycle analysis of H_2O_2-induced apoptosis in AT II cells. AT II cells were treated with 50 μM H_2O_2 in the presence or absence of caspase inhibitors (zVAD-fmk or caspase 3 inhibitor IV, 10 μM), or lysosomal proteinase inhibitors (the Cathepsin D inhibitor, Pepstatin A; or cathepsin B inbibitor II; 10 μM). The number of cells with sub-G1 DNA content was measured by flow cytometry 16 h after addition of H_2O_2.

Sixty minutes after addition of H_2O_2 only $15 \pm 7\%$ of the cells were in the positive range (Fig. 3). Cytochrome *c* release, assessed by immunoblotting analysis of the cytosolic fractions, was only observable 2 h after addition of H_2O_2 (Fig. 4). Importantly, both the induction of MMP and the release of cythocrome c observed in H_2O_2-treated cells were significantly attenuated in cells pre-treated with Pepstatin A (Figs. 3 and 4) (DiOC6 $49 \pm 15\%$, $P < 0.05$).

Lysosomal Disruption in H_2O_2 Treated AT II Cells

To examine the effect of H_2O_2 on lysosomal membrane stability AT II cells were loaded with acridine orange (AO), challenged with H_2O_2 and then the fluorescence of AO was measured by flow cytometry. AO is a weak base that, due to proton trapping, preferentially distributes within the acidic vacuolar lysosomal cellular

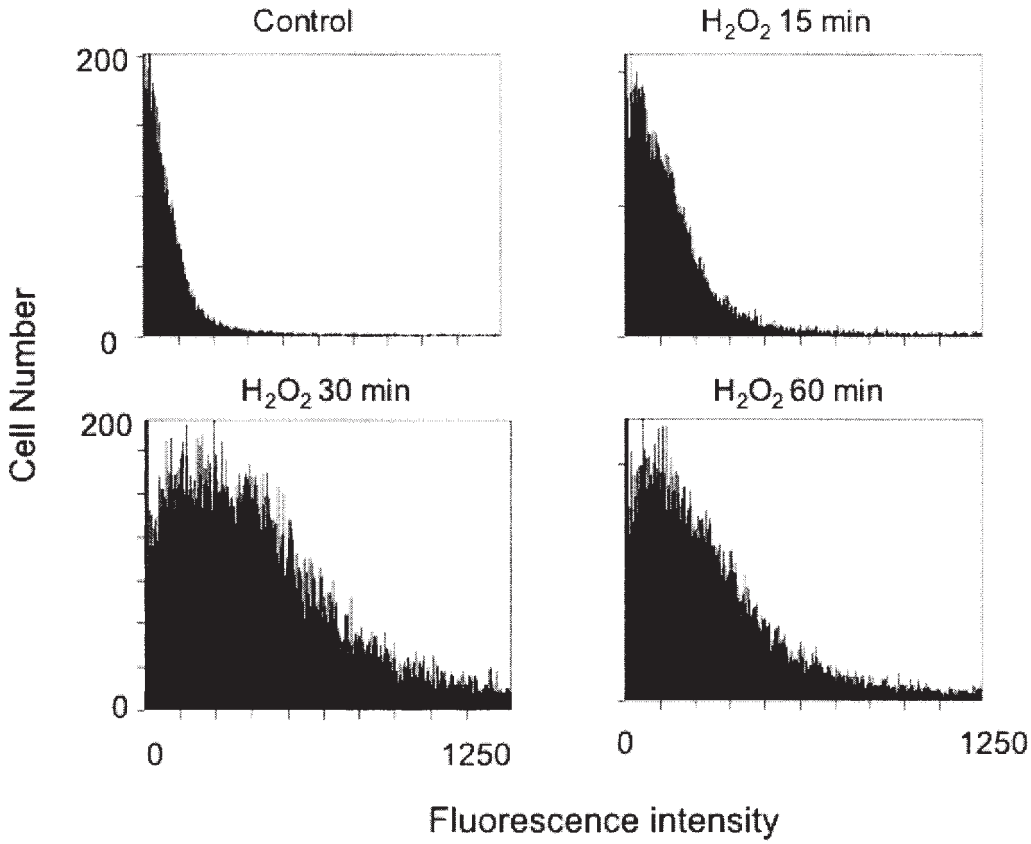

Fig. 2. Time course of increase in intracellular oxidants in H_2O_2-treated alveolar type II cells. Cells were loaded with DCFH-DA, washed and treated with 50 μM H_2O_2. DCF fluorescence was measured in untreated control cells, and 15, 30, and 60 min after addition of H_2O_2.

compartment. If lysosomal disruption occurs AO will accumulate in the cytoplasm, where due to differences in pH, will display green fluorescence. Untreated control cells showed only $3 \pm 2\%$ cells containing green fluorescent probe (Fig. 5). After H_2O_2-treatment there was a significant increase in the accumulation of cytoplasmic AO at 30 ($45 \pm 7\%$, $P < 0.05$) and 60 ($80 \pm 10\%$, $P < 0.01$) minutes. Pretreatment of cells with Pepstatin A prevented accumulation of cytoplasmic AO to only $50 \pm 14\%$ of the cells ($P < 0.05$ compared to H_2O_2 at 60 min).

Mitochondria and Lysosomal Changes in Live AT II Cells

To confirm the previous findings in non-fixed cells we conducted confocal microscopy studies of changes in markers of lysosomal and mitochondrial alterations in live AT II cells.

To measure lysosomal stability we used a pepstatin A BODIPY FL conjugate. In live cells, pepstatin A BODIPY FL is internalized and transported to lysosomes where due to the acidic pH it displays green fluorescence. Pepstatin A binds to cathepsin D and therefore can be used as a tracer of lysosomal rupture. Release of pepstatin A BODIPY FL–cathepsin D complexes into the cytosol, where the pH is neutral, is visualized as a decrease in green fluorescence [Chen et al., 2000]. Our data show that H_2O_2 treatment induces lysosomal disruption (Fig. 6, first column). The loss of green fluoresence is already evident 30 min after addition of H_2O_2 and almost total at 60 min (Fig. 6).

To visualize changes in mitochondrial membrane potential we used MitoTracker Red CMXRos, a cell-permeant, mitochondrion-selective probe that provides reliable detection of the loss of mitochondrial membrane potential [Gilmore and Wilson, 1999]. In agreement with the results in fixed cells (Fig. 3), we found that in live cells, H_2O_2 treatment induces a noticeable drop in mitochondrial membrane potential (Fig. 6, second column). The drop in

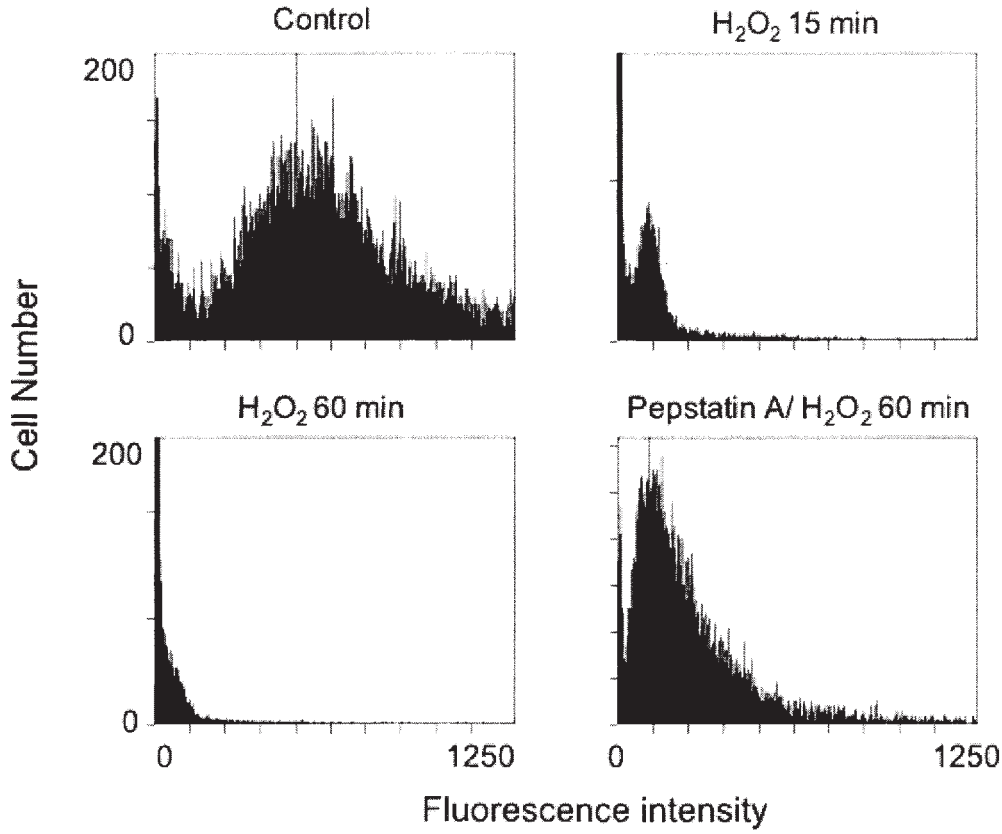

Fig. 3. Mitochondria membrane potential changes in H_2O_2-treated AT II cells. Untreated control cells and H_2O_2-treated cells were loaded with DIOC6 as described in Materials and Methods and the loss of green fluorescence was followed by flow cytometry. Where indicated Pepstatin A was added to the culture medium 2 h prior to addition of 50 μM H_2O_2.

MitoTracker Red fluorescence followed the time of treatment, being noticeable at 30 min and more evident 60 min after addition of H_2O_2 (Fig. 6).

Of note, there was a significant reduction in cell size in the early stages of H_2O_2-induced apoptosis (within 30 min, Fig. 6) as compared to the relatively constant size of the nucleus, a characteristic feature of apoptotic cell death.

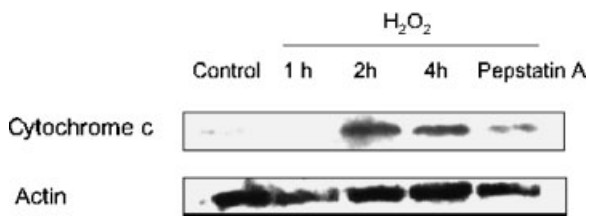

Fig. 4. Cytochrome *c* release after H_2O_2 treatment. Cytochrome *c* was measured in cytosolic extracts from untreated controls and H_2O_2-treated cells using specific polyclonal antibodies. Where indicated Pepstatin A was added to the culture medium 2 h prior to addition of 50 μM H_2O_2. The lower panel shows equal loading. The gel is representative of three independent experiments.

Ultrastructural Changes in H_2O_2-Treated AT II Cells

Addition of H_2O_2 to the culture medium of primary AT II cells led to morphological changes consistent with apoptosis (Fig. 7). AT II cells exposed to H_2O_2 for 16 h showed marked cellular shrinkage, chromatin condensation, mitochondrial matrix rarefaction, and separation of cristae (moderate swelling), cytoplasmic disruption, and cell membrane blebbing (Fig. 7D). Although the full apoptotic morphology developed after 8 h of exposure, some early signs of cellular dysfunction were already noticeable at shorter times. One hour after H_2O_2 addition mitochondria showed early swelling and there were some signs of cytoplasmic disruption, but the nuclei were intact and cell size was preserved (Fig. 7B). Four hours after treatment there was visibly increased activity

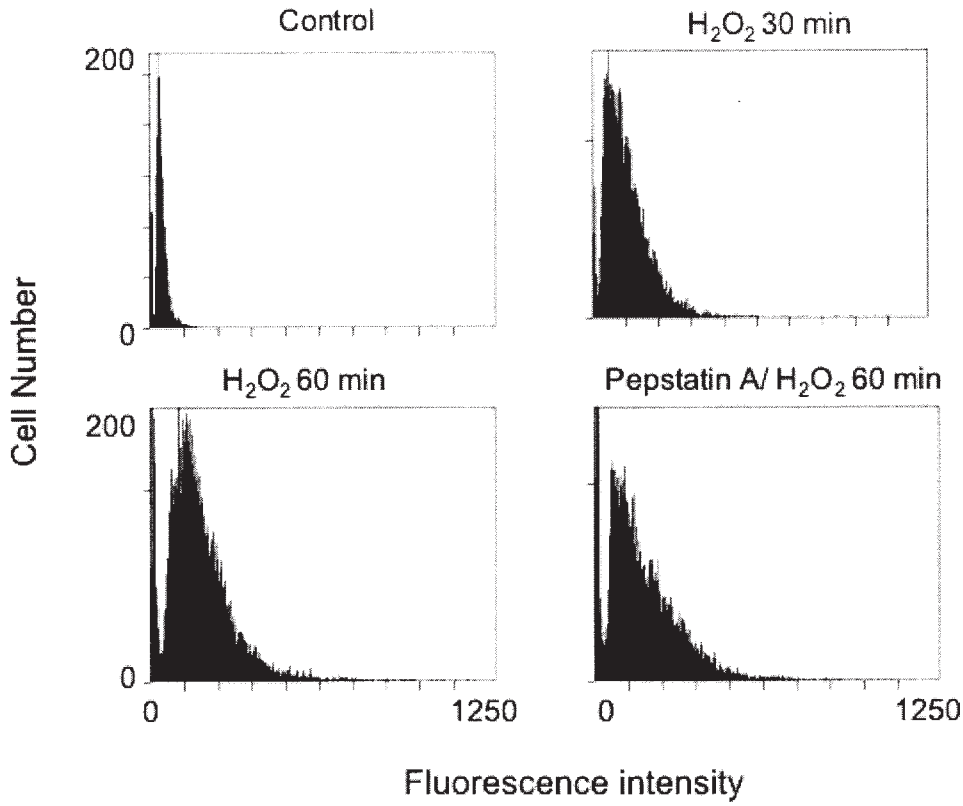

Fig. 5. Changes in lysosomal membrane stability in H_2O_2-treated AT II cells. Untreated control cells and H_2O_2-treated cells were loaded with acridine orange (AO) as described in Materials and Methods and the increase in green fluorescence intensity was followed by flow cytometry. Where indicated Pepstatin A was added to the culture medium 2 h prior to addition of 50 μM H_2O_2.

in the endoplasmic reticulum, moderate mitochondrial swelling, and observable membrane blebbing (Fig. 7C). The nuclei appeared intact and there was no change in cell volume.

Pre-treatment of AT II cells with pepstatin A prevented the development of the apoptotic features. Pepstatin A-treated cells showed normal nuclei and mitochondria, lesser cytoplasmic disruption and blebbing, and higher ER activity (Fig. 7E).

DISCUSSION

Lung epithelial cells are major targets for oxidant injury. The survival of functional AT II cells is critical to ensure efficient repair of the damaged alveolar surface after injury. Depending on the environmental signals, AT II cells can remain quiescent or proceed toward proliferation or apoptosis. Apoptosis may be important for the resolution or promotion of carcinogenesis or other proliferative diseases [Manning and Patierno, 1996] but the signaling pathways modulating apoptotic changes in AT II cells are still poorly defined. Our results show that acute exposure to H_2O_2 leads to significant increases in intracellular oxidants and in the percentage of apoptotic AT II cells. We found that H_2O_2-induced apoptosis in primary AT II cells is regulated through signaling pathways that involve both lysosomal and mitochondrial alterations. Lysosomal rupture occurred almost simultaneously with mitochondrial destabilization. However, inhibition of specific lysosomal proteolytic activities (cathepsin D) prevented cytochrome *c* release and mitochondrial membrane permeabilization as well as the development of AT II cell apoptosis, suggesting that lysosomal rupture is necessary for the activation of the mitochondrial pathway of cell death.

Although there is consensus that the "central executioner" of apoptosis involves mitochondrial membrane permeabilization and/or direct activation of the caspase cascade, the pathways leading to these events vary for different cell types and under different types of stress.

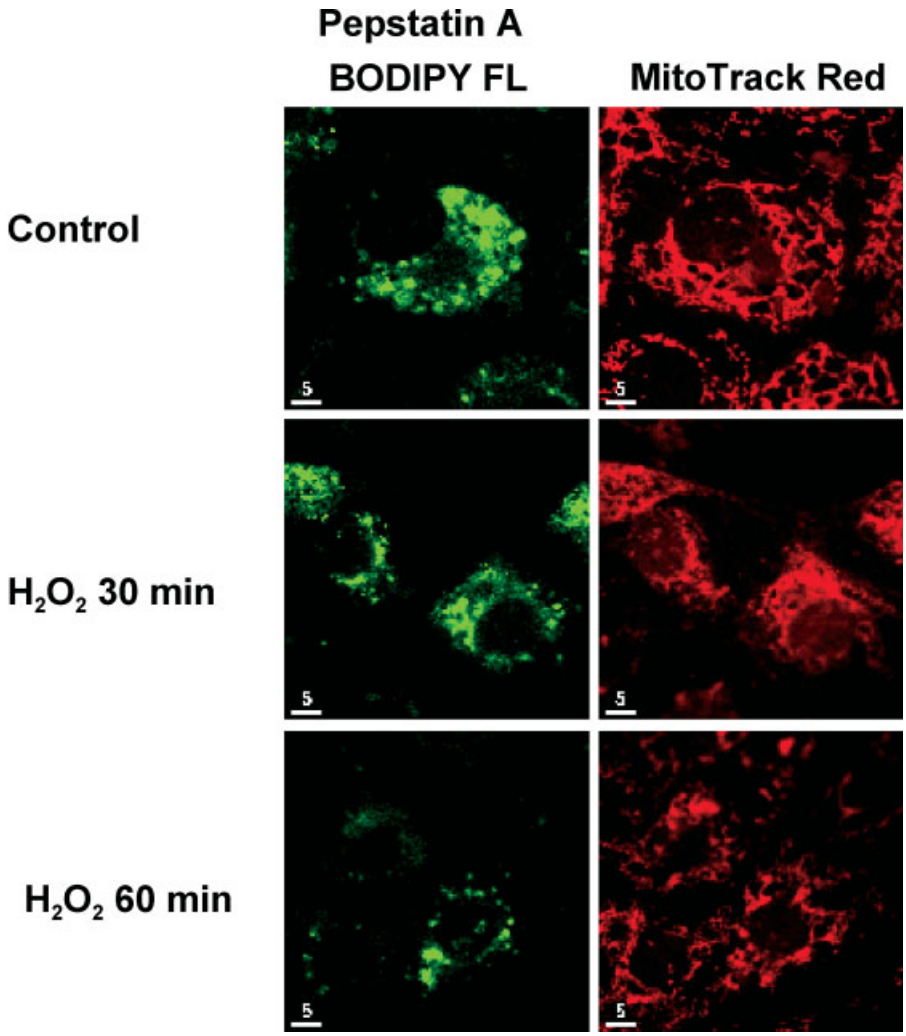

Fig. 6. Mitochondrial and lysosomal alterations in living AT II cells after H_2O_2 treatment. Cells were loaded with pepstatin A BODIPY® FL conjugate and MitoTracker Red as described in Materials and Methods. Release of lysosomal cathepsin D and decreases in mitochondrial membrane potential were measured 30 and 60 min after addition of 50 μM H_2O_2. Noticeable cell shrinkage and loss of green and red fluorescence is observable shortly after H_2O_2 treatment. The bars in the lower left corner of each figure corresponds to 5 μm. The images are representative of three independent experiments.

Accumulating evidence suggest organelle-specific initiation steps of the cell death pathway [Ferri and Kroemer, 2001]. Here we show that, in AT II cells, lysosomal rupture precedes and is required for mitochondrial destabilization and apoptosis.

H_2O_2-induced apoptosis was totally prevented by blockage of the caspase cascade with the broad-spectrum inhibitor zVAD-fmk, and almost completely inhibited by a caspase 3 inhibitor, indicating a significant involvement of the caspases cascade. Our results are in agreement with the observation that none of the executioner caspases seem to fully control execution of all the aspects of apoptosis [Degterev et al., 2003]. Instead, different caspases seem to have critical roles in specific pathways, and redundant functions in the majority of the general apoptotic events. Therefore, inhibition of all caspases is required to observe complete inhibition of all apoptotic features.

The apoptotic signaling pathways that lead to caspase activation can be subdivided into two major categories: cell surface sensor-mediated and intracellular sensor-mediated. Both require signal amplification through mitochondrial damage [Degterev et al., 2003]. Although caspase proteases are well-established effectors of apoptotic pathways, evidence has accumulated in recent years that non-caspases, including cathepsins, calpains, granzymes, and the proteasome complex, also have roles in mediating

and promoting cell death. Cathepsins are hypothesized to mediate apotosis by cleaving cytosolic substrates such as caspases [Schotte et al., 1998; Hishita et al., 2001], Bid [Stoka et al., 2001; Cirman et al., 2004], or phospholipase A [Brunk et al., 2001], or direct attack on the nucleus [Vancompernolle et al., 1998], or on mitochondrial or lysosomal membranes with the concomitant release of pro-apoptotic factors and more lysosomal enzymes [Brunk et al., 2001]. Taken together these findings point out to a extensive cross-talk between the mitochondrial and lysosomal pathways of cell death.

In our system, AT II cell apoptosis by H_2O_2 was partially prevented by inhibition of cathepsin B and completely blocked by inhibition of cathepsin D inhibitor (Fig. 1). Cathepsin B, an abundant and ubiquitous lysosomal cysteine peptidase, contributes significantly to TNF-alpha induced hepatocyte apoptosis [Guicciardi et al., 2000, 2001]. However, changes in its cytoplasmic levels do not correlate with changes in the development of apoptosis in human tumor HeLa cells [Gewies and Grimm, 2003]. Furthermore, cathepsin B was found to be an anti-apoptotic factor in neuronal cells [Uchiyama,

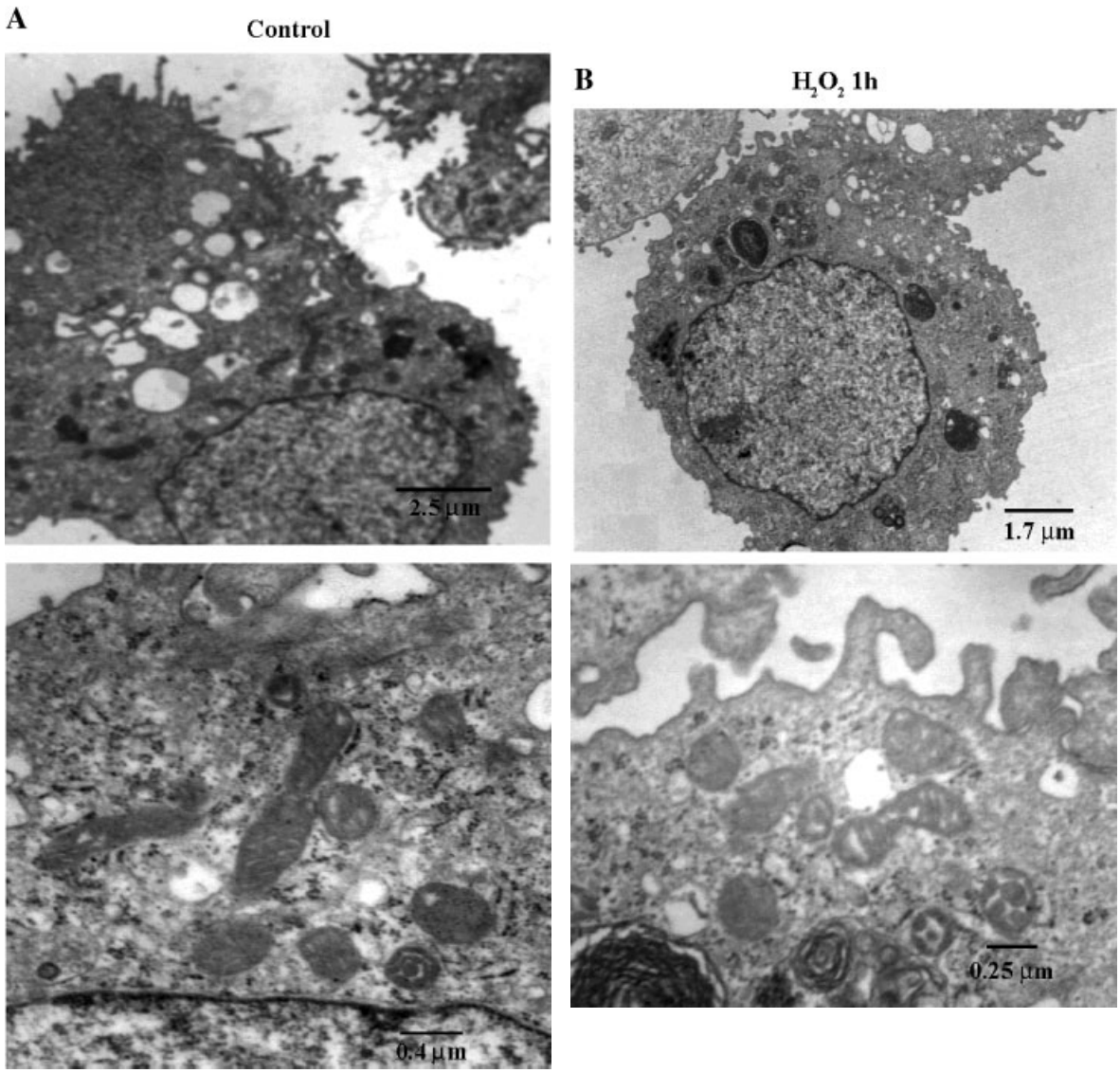

Fig. 7. Ultrastructural changes in H_2O_2-treated AT II cells. Control and Pepstatin A-treated AT II cell were added with 50 μM H_2O_2 and incubated at 37°C. At the indicated times, cells were spun down, fixed, and prepared for electron microscopy as described in Materials and Methods. The upper row shows low magnification pictures for each group. The lower row shows higher magnification images to visualize the morphological alterations in organelles. Magnifications are indicated in the lower left corner of each image.

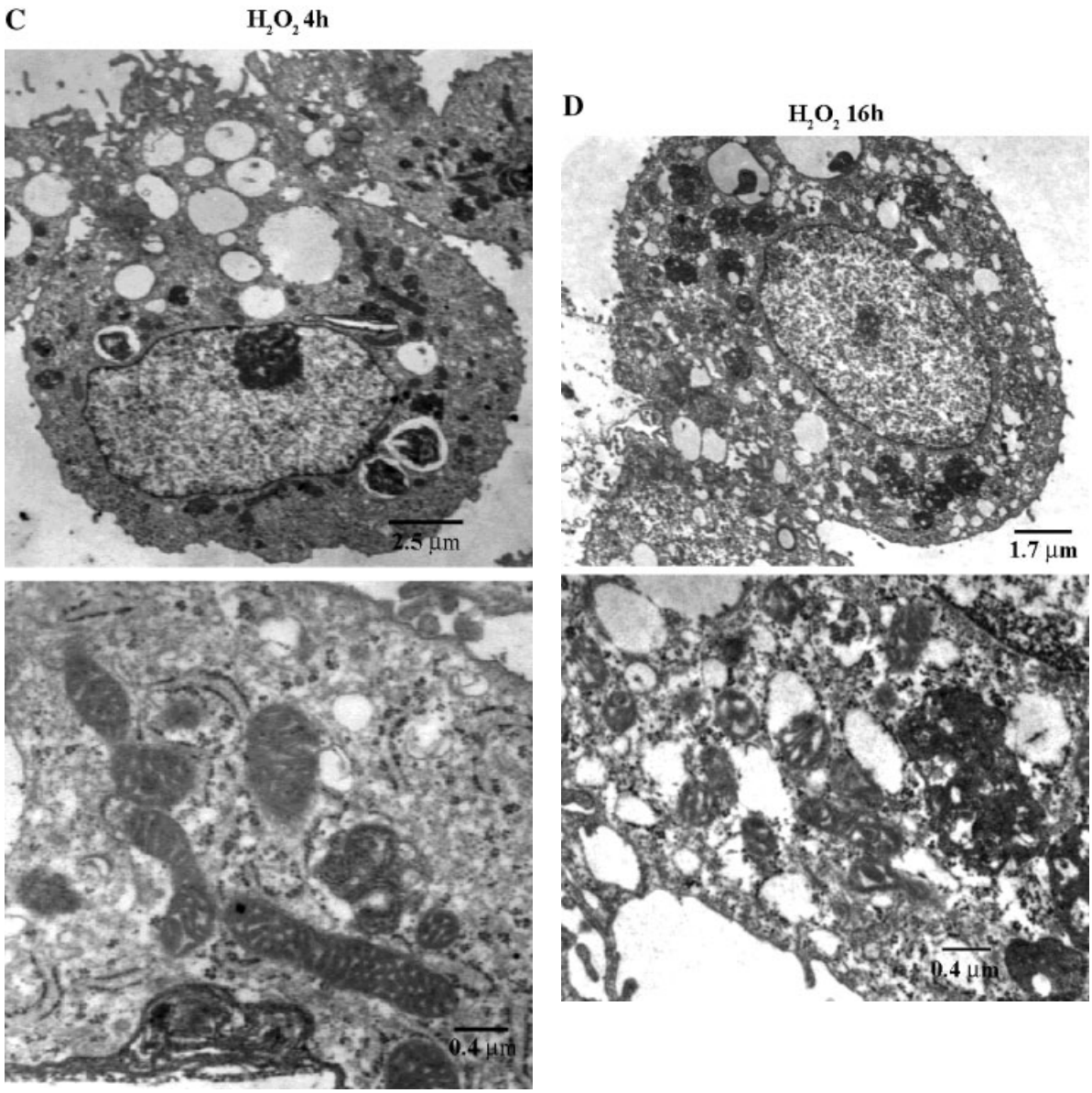

Fig. 7. (*Continued*)

2001]. Cathepsin D, a major intracellular aspartyl protease, is a mediator of IFN-gamma and TNF-alpha induced apoptosis [Tsukuba et al., 2000]. Cathepsin D levels show a positive correlation with apoptosis in neuronal cells [Uchiyama, 2001]. Cathepsin D has been shown to mediate apoptosis induced by the pro-oxidant naphthazarine [Kagedal et al., 2001]. Our data indicate that, in lung epithelial cells, both cathepsin B and D are pro-apoptotic signals.

There is also evidence that initiation of apoptosis by non-oxidant compounds involve the early release of cathepsins B and D, activation of PLA_2, and increased production of mitochondrial oxidants [Zhao et al., 2003]. Our data showing that cathepsin D inhibition prevents H_2O_2-initiated MMP and release of cytochrome *c* (Figs. 3 and 4) strongly suggests direct effects on the mitochondrial membrane. Interestingly, the partial prevention of lysosomal rupture by Pepstatin A (Fig. 5) also suggests that to some extent lysosomal enzymes directly attack the lysosomes.

Oxidant-induced apoptosis of lung cells is important to the pathology of hyperoxic injury [Mantell and Lee, 2000; Wang et al., 2003],

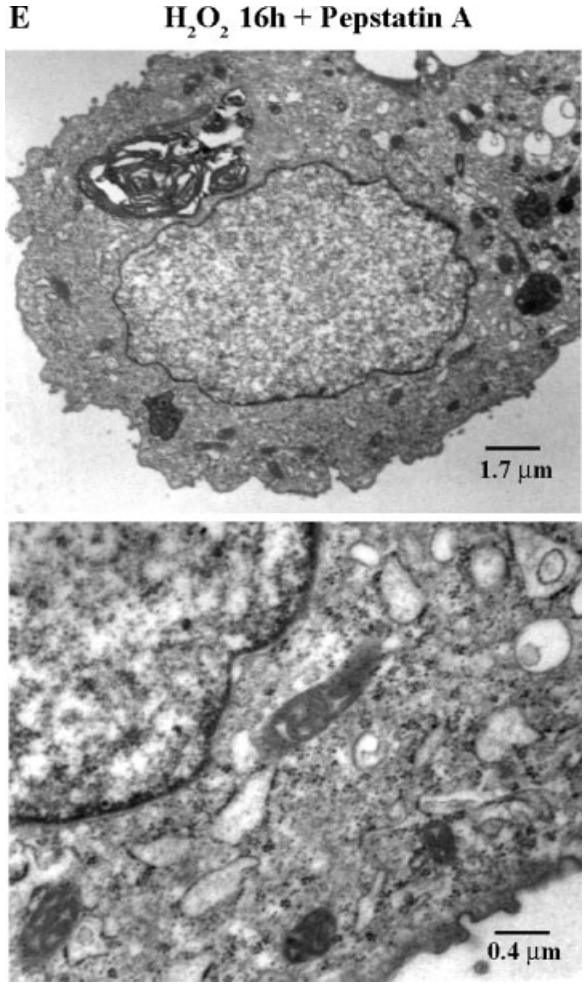

Fig. 7. (*Continued*)

emphysema [Tuder et al., 2003], and the toxic responses to cigarette smoke [Carnevali et al., 2003]. Apoptosis is also a major pathway for the resolution of AT II cells after acute lung injury [Bardales et al., 1996]. Our data suggests that pharmacological inhibition of lysosomal rupture may prove effective in the treatement of oxidant-induced lung injury.

ACKNOWLEDGMENTS

We thank Ms. A. Imrich, and Dr. Yao Yu Ning for assistance in the determinations of apoptosis by flow cytometry, and to Ms. Jean Lai for assistance with the confocal microscopic evaluation of cells.

REFERENCES

Antunes F, Cadenas E, Brunk UT. 2001. Apoptosis induced by exposure to a low steady-state concentration of H_2O_2 is a consequence of lysosomal rupture. Biochem J 356:549–555.

Bardales RH, Xie SS, Schaefer RF, Hsu SM. 1996. Apoptosis a major pathway responsible for the resolution of type II pneumocytes in acute lung injury. Am J Pathol 149:845–852.

Bass DA, Parce JW, Dechatelet LR, Szejda P, C SM, Thomas M. 1983. Flow cytometric studies of oxidative product formation by neutrophils: A graded response to membrane stimulation. J Immunol 130:1910–1917.

Brookes PS, Levonen AL, Shiva S, Sarti P, Darley-Usmar VM. 2002. Mitochondria: Regulators of signal transduction by reactive oxygen and nitrogen species. Free Radic Biol Med 33:755–764.

Brunk UT, Zhang H, Dalen H, Ollinger K. 1995. Exposure of cells to nonlethal concentrations of hydrogen peroxide induces degeneration-repair mechanisms involving lysosomal destabilization. Free Radic Biol Med 19: 813–822.

Brunk UT, Neuzil J, Eaton JW. 2001. Lysosomal involvement in apoptosis. Redox Rep 6:91–97.

Carnevali S, Petruzzelli S, Longoni B, Vanacore R, Barale R, Cipollini M, Scatena F, Paggiaro P, Celi A, Giuntini C. 2003. Cigarette smoke extract induces oxidative stress and apoptosis in human lung fibroblasts. Am J Physiol Lung Cell Mol Physiol 284:L955–L963.

Carvalho H, Evelson P, Sigaud S, González-Flecha B. 2004. Mitogen-activated protein kinases modulate H_2O_2-induced apoptosis in primary rat alveolar epithelial cells. J Cell Biochem 92:502–513.

Chen YR, Wang X, Templeton D, Davis RJ, T.H T. 1996. The role of c-Jun N-terminal kinase (JNK) in apoptosis induced by ultraviolet C and gamma radiation. Duration of JNK activation may determine cell death and proliferation. J Biol Chem 271:31929–31936.

Chen CS, Chen WN, Zhou M, Arttamangkul S, Haugland RP. 2000. Probing the cathepsin D using a BODIPY FL-pepstatin A: Applications in fluorescence polarization and microscopy. J Biochem Biophys Methods 42:137–151.

Cirman T, Oresic K, Mazovec GD, Tirk V, Reed JC, Myers RM, Salvesen GS, Turk B. 2004. Selective disruption of lysosomes in HeLa cells triggers apoptosis mediated by cleavage of Bid by multiple papain-like lysosomal cathepsins. J Biol Chem 279:3578–3587.

Dare E, Li W, Zhivotovsky B, Yuan X, Ceccatelli S. 2001. Methylmercury and H(2)O(2) provoke lysosomal damage in human astrocytoma D384 cells followed by apoptosis. Free Radic Biol Med 30:1347–1356.

Degterev A, Boyce M, Yuan J. 2003. A decade of caspases. Oncogene 22:8543–8567.

Dobbs LG. 1990. Isolation and culture of alveolar type II cells. Am J Physiol 258:L134–L147.

Ferri KF, Kroemer G. 2001. Organelle-specific initiation of cell death pathways. Nat Cell Biol 3:E255–E263.

Gewies A, Grimm S. 2003. Cathepsin-B and cathepsin-L expression levels do not correlate with sensitivity of tumour cells to TNF-alpha-mediated apoptosis. Br J Cancer 89:1574–1580.

Gilmore K, Wilson M. 1999. The use of chloromethyl-X-rosamine (Mitotracker red) to measure loss of mitochondrial membrane potential in apoptotic cells is incompatible with cell fixation. Cytometry 36:355–358.

González-Flecha B, Evelson P, Ridge K, Sznajder JI. 1996. Hydrogen peroxide increases Na+/K(+)-ATPase function in alveolar type II cells. Biochimica et Biophysica Acta 1290:46–52.

Guicciardi ME, Deussing J, Miyoshi H, Bronk SF, Svingen PA, Peters C, Kaufmann SH, Gores GJ. 2000. Cathepsin B contributes to TNF-alpha-mediated hepatocyte apoptosis by promoting mitochondrial release of cytochrome c. J Clin Invest 106:1127–1137.

Guicciardi ME, Miyoshi H, Bronk SF, Gores GJ. 2001. Cathepsin B knockout mice are resistant to tumor necrosis factor-alpha-mediated hepatocyte apoptosis and liver injury: Implications for therapeutic applications. Am J Pathol 159:2045–2054.

Gurgueira SA, Lawrence J, Coull B, Krishna Murthy GG, González-Flecha B. 2002. Rapid increases in the steady-state concentration of reactive oxygen species in the lungs and heart after particulate air pollution inhalation. Environ Health Perspect 110:749–755.

Hishita T, Tada-Oikawa S, Tohyama K, Miura Y, Nishihara T, Tohyama Y, Yoshida Y, Uchiyama T, Kawanishi S. 2001. Caspase-3 activation by lysosomal enzymes in cytochrome c-independent apoptosis in myelodysplastic syndrome-derived cell line P39. Cancer Res 61:2878–2884.

Janssen YM, Matalon S, Mossman BT. 1997. Differential induction of c-fos, c-jun, and apoptosis in lung epithelial cells exposed to ROS and RNS. Am J Physiol 273:L789–L796.

Kagedal K, Johansson U, Ollinger K. 2001. The lysosomal cathepsin D mediates apoptosis induced by oxidative stress. FASEB J 15:1592–1594.

Kelly FJ, Lubec G. 1995. Hyperoxic injury of immature guinea pig lung is mediated via hydroxyl radicals. Pediatr Res 38:286–291.

Manning FC, Patierno SR. 1996. Apoptosis: Inhibitor or instigator of carcinogenesis?. Cancer Invest 14:455–465.

Mantell LL, Lee PJ. 2000. Signal transduction pathways in hyperoxia-induced lung cell death. Mol Gen Metabol 71: 35–70.

Nishino H, Nemoto N, Lu W, Sakurai I. 1999. Significance of apoptosis in morphogenesis of human lung development: Light microscopic observation using in situ DNA end-labeling and ultrastructural study. Med Electron Microsc 32:57–61.

Pervaiz S, Seyed MA, Hirpara JL, Clement MV, Loh kW. 1999. Purified photoproducts of merocyanide 540 trigger cytochrome c release and caspase 8-dependent apoptosis in human leukemia and melanoma cells. Blood 93:4096–4108.

Ryrfeldt A, Bannenberg GPM. 1993. Free radicals and lung disease. Br Med Bull 49:588–603.

Schotte P, Van Criekinge W, Van de Craen M, Van Loo G, Desmedt M, Grooten J, Cornelissen M, De Ridder L, Vandekerckhove J, Fiers W, Vandenabeele P, Beyaert R. 1998. Cathepsin B-mediated activation of the proinflammatory caspase-11. Biochem Biophys Res Commun 251: 379–387.

Sigaud S, Evelson P, González-Flecha B. 2004. H_2O_2-induced proliferation of primary alveolar epithelial cells is mediated by MAP kinases. Antioxidants Redox Signaling (in press).

Stoka V, Turk B, Schendel SL, Kim TH, Cirman T, Snipas SJ, Ellerby LM, Bredesen D, Freeze H, Abrahamson M, Bromme D, Krajewski S, Reed JC, Yin XM, Turk V, Salvesen GS. 2001. Lysosomal protease pathways to apoptosis. Cleavage of bid, not pro-caspases, is the most likely route. J Biol Chem 276:3149–3157.

Tsukuba T, Okamoto K, Yasuda Y, Morikawa W, Nakanishi H, Yamamoto K. 2000. New functional aspects of cathepsin D and cathepsin E. Molecules Cells 10:601–611.

Tuder RM, Zhen L, Cho CY, Taraseviciene-Stewart L, Kasahara Y, Salvemini D, Voelkel NF, Flores SC. 2003. Oxidative stress and apoptosis interact and cause emphysema due to vascular endothelial growth factor receptor blockade. Am J Respir Cell Mol Biol 29:88–97.

Uchiyama Y. 2001. Autophagic cell death and its execution by lysosomal cathepsins. Arch Histol Cytol 64:233–246.

Vallyathan V, Shi X. 1997. The role of oxygen free radicals in occupational and environmental lung diseases. Environ Health Perspect 105:165–177.

Vancompernolle K, Van Herreweghe F, Pynaert G, Van de Craen M, De Vos K, Totty N, Sterling A, Fiers W, Vandenabeele P, Grooten J. 1998. Atractyloside-induced release of cathepsin B, a protease with caspase-processing activity. FEBS Lett 438:150–158.

Wang X, Ryter SW, Dai C, Tang ZL, Watkins SC, Yin XM, Song R, Choi AM. 2003. Necrotic cell death in response to oxidant stress involves the activation of the apoptogenic caspase-8/bid pathway. J Biol Chem 278:29184–29191.

Ye J, Wang S, Leonard SS, Sun Y, Butterworth L, Antonini J, Ding M, Rojanasakul Y, Vallathan V, Castranova V, Shi X. 1999. Role of reactive oxygen species and p53 in chromiun(VI)-induced apoptosis. J Biol Chem 274: 34974–34980.

Zhao M, Antunes F, Eaton JW, Brunk UT. 2003. Lysosomal enzymes promote mitochondrial oxidant production, cytochrome c release, and apoptosis. Eur J Biochem 270:3778–3786.